



Swansea University
Prifysgol Abertawe



Cronfa - Swansea University Open Access Repository

This is an author produced version of a paper published in:
Advanced Materials Technologies

Cronfa URL for this paper:
<http://cronfa.swan.ac.uk/Record/cronfa40885>

Paper:

De Rossi, F., Baker, J., Beynon, D., Hooper, K., Meroni, S., Williams, D., Wei, Z., Yasin, A., Charbonneau, C., et. al. (2018). All Printable Perovskite Solar Modules with 198 cm² Active Area and Over 6% Efficiency. *Advanced Materials Technologies*, 1800156
<http://dx.doi.org/10.1002/admt.201800156>

This item is brought to you by Swansea University. Any person downloading material is agreeing to abide by the terms of the repository licence. Copies of full text items may be used or reproduced in any format or medium, without prior permission for personal research or study, educational or non-commercial purposes only. The copyright for any work remains with the original author unless otherwise specified. The full-text must not be sold in any format or medium without the formal permission of the copyright holder.

Permission for multiple reproductions should be obtained from the original author.

Authors are personally responsible for adhering to copyright and publisher restrictions when uploading content to the repository.

<http://www.swansea.ac.uk/library/researchsupport/ris-support/>

DOI: 10.1002/ ((please add manuscript number))

Article type: full paper

All printable perovskite solar modules with 198 cm² active area and over 6% efficiency

*Francesca De Rossi, Jenny Baker, Dave Beynon, Katherine Hooper, Simone Meroni, Daniel Williams, Zhengfei Wei, Amrita Yasin, Cecile Charbonneau, Eifion Jewell, and Trystan M. Watson**

Dr. F. De Rossi, Dr. J. Baker, Dr. D. Beynon, Dr. K. Hooper, S. Meroni, D. Williams, Dr. Z. Wei, Dr. A. Yasin, Dr. C. Charbonneau, Dr. E. Jewell, and Prof. T. M. Watson
Swansea University Bay Campus, Fabian Way, SA1 8EN, Swansea, UK
E-mail: T.M.Watson@swansea.ac.uk

Keywords: perovskite solar cells, modules, carbon, mesoporous, printed

Perovskite solar cells based on an all printable mesoporous stack, made of overlapping titania, zirconia and carbon layers, represent a promising device architecture for both simple, low cost manufacture and outstanding stability. Here a breakthrough in the upscaling of this technology is reported: screen printed modules on A4 sized FTO-glass substrates, delivering power conversion efficiency (PCE) ranging from 3 to 5% at 1 sun on an unprecedented 198 cm² active area. An increase in the PCE, due to higher V_{OC} and fill factor, is demonstrated by patterning the TiO₂ blocking layer. Furthermore, an unexpected increase of the performance is observed over time, while storing the modules in the dark, un-encapsulated, at ambient conditions (with humidity increasing from 30 and 70% RH), resulting in 6.6% PCE and 6.3% stabilised at V_{max} measured after over 2 months since fabrication. Equally impressive is the low light performance with 11% and 18% PCE achieved respectively at 200 and 1000 lux under fluorescent lighting. It is hoped that this demonstration of good performance on large area can unlock the viability of perovskite solar cells manufactured on an industrial scale.

1. Introduction

Among the different cell architectures for perovskite solar cells (PSCs), carbon-based HTM-free PSCs (C-PSCs) seem to be the most promising for addressing stability issues and tackling

the up-scaling challenges by combining ease of manufacture with low cost of materials.^[1, 2, 3] Although lagging behind other PSC types in terms of record efficiency on lab scale cells (~17%^[4] vs over 22% for a mesoporous TiO₂/perovskite/PTAA/Au^[5]), C-PSCs have demonstrated over 1000 hours stability under different conditions of illumination and external stresses, even un-encapsulated, when 5-ammonium valeric acid iodide (5-AVAI) is added to the perovskite solution.^[6, 7, 8] Since the entire triple mesoporous stack – titania (m-TiO₂), zirconia (ZrO₂), carbon (C) - is printable, C-PSCs are ideal for large scale production and, interestingly, some features that prevent degradation, i.e. lack of metal cathode^[9] and organic HTM^[10], are also responsible for the simpler manufacturing process, paving the way for C-PSCs to move quickly from the lab to the market. This module architecture not only uses low cost materials but can be produced by equipment that has a very low capital cost thus reducing the barrier to commercialisation of perovskite modules. Constraining the grain growth of the perovskite completely within the three mesoporous structures enables crystallisation of the perovskite over large areas without the need for dynamic drying^[11, 12] to mimic the spin coating process.^[13]

There have been some reports demonstrating that C-PSC modules can be produced by screen printing, via registration of the overlapping layers, and can deliver between 10 and 11% PCE on 10 x 10 cm² substrates, with active areas ranging from 47.6 cm²^[7, 14] to 70 cm²^[15], and, in particular, showing over 1 year stability under illumination, as reported by Grancini et al.^[7]

These results for C-PSC modules are even more remarkable, considering that modules with comparable active areas (>45 cm²) and different device architecture, yielded respectively 12.6% PCE on 50.6 cm² (FTO/c-TiO₂/graphene+m-TiO₂/GO-Li/perovskite/spiro-OMeTAD/Au)^[16], 8.7% PCE on 60 cm² (ITO/PEDOT:PSS/MAPI/PCBM/Au)^[17], and 4.3% PCE on 100 cm² (FTO/c-TiO₂/m-TiO₂/perovskite/spiro-O-MeTAD/Au)^[11]; moreover, the

record for PSC modules overall is Microquanta's 16% PCE^[18, 19] on just 16.29 cm² aperture area (active area + dead area for interconnections).

Up-scaling C-PSC manufacture from 10 x 10 cm² to larger substrate dimensions, e.g. A4 size as in our case, is far from trivial. Spraying the TiO₂ blocking layer (BL) at temperatures as high as 300 °C causes the large substrates to crack in the worst case or to bend, compromising the thickness homogeneity over the substrate of the printed layers, mostly and more crucially for the thinnest of the three, the sub-micrometric m-TiO₂. Any change in the layers' thickness across the substrate can affect the performance of individual cells constituting the module and, in series connected modules, the worst cell will dictate the overall performance of the device. Thus, a lower processing temperature is needed for depositing the BL while ensuring it is still endowed with blocking properties and the conductive glass substrate is not deformed afterwards, affecting the printing process; also, an optimisation of the printing settings is crucial to ensure a consistent distribution of each layer's thickness across the whole substrate.

Herein we demonstrate that, with this optimisation, A4-size modules with an active area of 198 cm² can be manufactured by screen printing, via registration of the overlapping layers. We confirm the need for patterning of the TiO₂ blocking layer to improve the interconnection between adjacent cells and thus module performance. We discuss the issues related to processing an A4-sized FTO glass substrate at high temperatures and how to obtain uniform printed layers on such large areas. We also report the unexpected performance improvement of un-encapsulated modules with storage time, likely related to humidity, leading to a remarkable 6.6% PCE (6.3% stabilised at V_{\max}) 2 months after fabrication.

2. Results and discussion

In this work, a conservative approach, based on the registration of the printed layers, was adopted to design the A4 size modules and achieve the series connection to adjacent cells. Though not effective in maximising the active area if compared to laser patterning^[20] or

mechanical scribing^[21], edge registration is a safe strategy to avoid short circuits and unintentional damage to underlayers. Each module consisted of 22 cells, 5 mm wide and 180 mm long, placed 6 mm apart one from the other (as shown in **Figure 1**), to guarantee 1.5 mm-wide ZrO₂ overlapping the m-TiO₂ on both sides and 3 mm-wide area for the series connection of the carbon top electrode to the adjacent cell's photoanode, resulting in 198 cm² active area, 435.6 cm² aperture area (active area + area for interconnections) and 45.5% geometrical fill factor (GFF, ratio between the active and the total area). Once the cell width and inter distance between cells were set at 5 and 3 mm respectively, cells' length and number of cells were maximised, given the full printable area of the screen, i.e. 200 x 250 cm². A cell width of 5 mm has been demonstrated to maximise the power output, based on the modelling and simulation of series connected PSC modules.^[22] The 3 mm-wide area for interconnections was chosen to minimise resistive losses due to the carbon electrode and to ensure an area large enough for the connection in series between two adjacent cells, without losing too much geometrical fill factor.

When working on large area substrates it is important to avoid unnecessary thermal stress which can cause distortion of the substrate making it difficult to get a homogeneous printing of the thin (i.e. 800 nm) m-TiO₂ across the large area. For this reason, the spraying of the compact TiO₂ blocking layer, both un-patterned and patterned, was carried out at 150 °C, rather than at 300 °C as per our standard fabrication method,^[23, 24] before printing the mesoporous TiO₂ and sintering both layers at 550 °C.

To compare the different processing temperatures, we sprayed BL films on FTO glass at 150 °C and 300 °C and characterised them, before and after sintering at 550 °C for 30 min. Morphological differences are appreciable in the SEM images in **Figure 2**: the BL sprayed at 150 °C (Figure 2-a) appears rougher than the one at 300 °C (Figure 2-c) and visually porous, even after sintering at 550 °C for 30 min (Figure 2-b and Figure 2-d, respectively), raising

questions about the effectiveness of its blocking properties. Furthermore, the BL sprayed at 300 °C after sintering at 550 °C did show the characteristic anatase peak in both Raman and XRD spectra (Figure 2-e and Figure 2-f), respectively at 145 cm⁻¹ and at 25.3 degrees, while the same peak was not detected in the BL sprayed at 150 °C, even after the sintering process.

It is likely that the porosity is due to the Ti-O matrix forming around some of the acetylacetonate ligands of the Ti precursor used, i.e. titanium di-isopropoxide bis(acetylacetonate) (TiAcAc). In the TiAcAc complex, acetylacetonate is in its anionic form bonded to the Ti⁴⁺, thus TiAcAc boiling temperature is slightly higher than that of acetylacetonate on its own (140 °C). When spraying on the substrate kept at 150 °C, some acetylacetonate ligands remain on the substrate for long enough to create the textured layer, shown in Figure 2, rather than the conformal compact layer obtained when the substrate is held at 300 °C. Such a TiO₂ framework formed at 150 °C possibly requires more energy to crystallize than is delivered at 550 °C, hence the lack of the characteristic anatase peak in both Raman and XRD spectra, even after sintering.

Despite the differences in TiO₂ morphology, the PV performance did not differ significantly for small C-PSC cells (0.25 cm² masked area) with BL sprayed at 150 °C or at 300 °C (Figure S1) and sintered afterwards at 550 °C so we inferred the method to be effective for large modules as well.

It is well known and accepted that the presence of the BL at the integrated vertical series interconnections between adjacent cells in a module leads to dramatic PCE drop, mainly due to poor FF^[25]; by patterning the BL, a direct contact between the bottom electrode (i.e. FTO) of each cell forming the module and the top electrode of the adjacent one (i.e. evaporated gold, or printed carbon in our case), is ensured, minimising the resistive losses, associated with the interconnections, and increasing the performance. The lift-off technique, successfully adopted by Matteocci et al. ^[25] for modules with 10 cm² active area, consists of a sintering

step at 450 °C for the metallic mask printed on the substrate and a bath in aqueous HCl solution to lift off the mask, steps we decided not to add to our fabrication process. Therefore, for patterning the BL, the FTO substrates were covered completely with Kapton tape, which was then laser cut and removed selectively to create a mask, covering the areas destined to become the interconnections only. After spraying the TiAcAc solution at 150 °C and prior to the following steps described in the experimental section, the adhesive mask was removed.

Beyond the blocking layer, the scale up to such a large size presented a challenge also during the printing stages, largely due to increased cohesive strength of the wet ink film with larger area coverage. Usually, when printing smaller areas that do not utilise the full printable area of the screen, the print speed and snap off (separation between screen and substrate, **Figure S2**) can be optimised at lower levels to ensure clean separation of the screen from the substrate following printing. In our case, the cohesive force, due to the large area of print coverage, manifested in slow separation of the screen from the substrate towards the end of the print stroke, resulting in a horseshoe shaped area of lower ink transfer (Figure S2), leading to inhomogeneous coverage. This was overcome through changing the settings relating to print speed and snap off: print speed was increased from 110 to 220 mm/s and snap off gap increased from 2.2 to 3.2 mm. This increase in speed and angle of screen separation enabled defect free printing of the large area modules.

Each layer's thickness was reasonably close to the nominal values (Figure 1), i.e. 800 nm for m-TiO₂, 1.2 µm for ZrO₂ and 10 µm for carbon, across the printed area, as confirmed by profilometry measurements for titania and zirconia layers (**Figure 3-a**) and by white light interferometry for the carbon electrode (Figure 3-b). The thin and 5 mm-wide TiO₂ layers presented a typical edge effect, common in printed thin films, which was measured as well and referred to as A_p to consider the different heights recorded at the edges and in the central part of the film. Thickness, average roughness and peak roughness for each layer were

measured in different zones of the A4 substrates (**Table S1**) to demonstrate the consistency across the whole printed area. Cross-section SEM/EDX images (**Figure 4**) also confirmed the layers' thickness and the elemental mapping of lead and iodine revealed that the perovskite infiltration was uniform and complete throughout the layers, despite a stack thickness of over 10 μm .

Modules with both un-patterned and patterned BLs were characterised under AM1.5 illumination, after soldering wires to the silver painted busbars to provide more robust electrical contacts, and the average PV parameters are reported in **Table 1**. As expected, modules with patterned BL gave better performance: 3.2% PCE (reverse scan) compared to 1.9% for the un-patterned BL, gaining about 20 mA of J_{SC} (from 78 to 91 mA) and 2 V of V_{OC} (from 16.3 to 18.2 V), as well as a 33% improvement in FF (from 29.2 to 38.9 %). To evaluate whether there is a margin for improvement, it is useful to compare these values measured for the modules to those of J_{SC} (~20-23 mA/cm²) and V_{OC} (~0.9-1 V) reported for best performing C-PSCs. A single strip in the module can be considered as an individual cell, whose V_{OC} is given by the module's V_{OC} divided by the number of cells in the module and whose J_{SC} is calculated as the module's I_{SC} divided by the active area of the single strip: in this way, un-patterned and patterned BL devices delivered poor J_{SC} , 8.7 and 10.1 mA/cm² respectively, and acceptable V_{OC} of 0.7 and 0.8 V, respectively.

Surprisingly, the same modules, kept in the dark without any encapsulation for 144 hours at ambient conditions, i.e. room temperature and 55% RH, did not degrade but improved, mainly in terms of photo-generated current (+26% and +18% for un-patterned and patterned BL respectively), suggesting some perovskite crystal re-arrangements and/or interface improvements. We believe the humidity in particular played a crucial role, as already suggested by Hashmi et al^[8], who demonstrated a performance improvement for C-PSCs, exposed to high humidity for over 200 h, and attributed it to an increase in perovskite

crystallite sizes, observed by XRD, as well as a TiO₂/perovskite interface more favourable for electron injection, as confirmed by PL measurements, and a more intimate contact between the perovskite and the porous carbon.

Thus, as a strategy to maximise potential PCE, the modules, after being stored for 144 hours in the dark at ambient conditions, were additionally exposed to 70% RH. As a result, after 48 hours at 70% RH in the dark, their PCE showed a further improvement of 21% and 31%, respectively for un-patterned and patterned BL, as shown in Table 1. Again, considering a single strip in the module as an individual cell, un-patterned and patterned BL devices, at this point, delivered respectively 10.9 and 12.2 mA/cm² of J_{SC} and 0.7 and 0.9 V of V_{OC}.

Low currents and fill factors can be ascribed to the still poor quality of either perovskite crystallisation, albeit uniformly infiltrated throughout the stack (see cross section SEM in Figure 4), or TiO₂/perovskite interface in terms of charge injection, or both, while recombination is the major contributor in reducing the V_{OC}, possibly due to the BL being not very compact, thus allowing some direct contact between perovskite and FTO. Comparing the modules' FF with best performing carbon cells, which can easily reach >60%, would be unfair as the design and quality of the interconnections between cells affect it significantly. Undoubtedly, patterning the BL resulted in both V_{OC} and FF improvement (18% and 45% respectively, for the reverse scan, after 144 hours at ambient conditions and 48 hours at 70% RH) and reduction of the series resistances, as shown in **Figure 5**, by the I-V curve slope around V_{OC}, which is much steeper for the module with patterned BL. The noticeable hysteresis is likely due to the modules' heating during the measurements (~66 sec per scan, >2 min per measurement, causing the glass side to reach 50-55 °C measured by a thermocouple), as temperature can increase ion migration inducing hysteresis.^[26, 27] It is also related to the slow response of perovskite materials upon illumination and to a light-induced

polarization, which can be explained by the build-up and discharge of mobile ions, affecting the interfacial recombination processes.^[28]

The observed FF improvement with BL patterning can be explained by the lower contact resistance, due to direct contact of one cell's carbon top electrode to the FTO of the adjacent cell, without any TiO₂ BL in-between. A lower contact resistance could reasonably reduce recombination, as charges transfer more easily from cell to cell, resulting in higher V_{OC}. The comparison between patterned BL (Carbon/FTO) and un-patterned BL (Carbon/BL/FTO) was carried out using TLM^[25] to extract parameters such as transfer length (L_T), contact resistivity (ρ_C) and contact resistance (R_C, using 540 mm² contact area), which are shown in the inset table in Figure 5. The contact resistivity (ρ_C) for Carbon/BL/FTO is equal to 147 Ω·mm², one order of magnitude higher than for Carbon/FTO (34 Ω·mm²), due to the presence of the blocking layer between Carbon and FTO (**Figure S3**). As a result, the contact resistance is 0.27 Ω and 0.06 Ω, respectively for Carbon/BL/FTO and Carbon/FTO. The transfer length, associated with the distance over which most of the current is transferred from the carbon electrode to the FTO, halves with patterning the BL, from 4.6 mm to 2.2 mm. This suggests an increase of the aperture ratio (active area/aperture area) for these modules is achievable, by reducing the contact area width from 3 to 2.2 mm.

Interestingly, the best module with patterned BL maintained its performance for over 288 hours at 70% RH as shown in **Figure S4**. It was then stored in a box with silica (~30% RH) and tested infrequently. After 528 hours following fabrication, it had reached almost 5% PCE, 19.6 V of V_{OC} (0.891 V per cell), 125 mA of I_{SC} (13.9 mA/cm²) and 40% FF. After 2 months following fabrication, it was tested again as a thermostatically controlled holder had become available and the effect of light soaking at open circuit on performance could be assessed. An improvement of all the PV parameters was observed, as reported in **Table 2**, with light soaking the module for 10 minutes at open circuit before running the measurements, as well

as a better shape for the I-V curves, as shown in **Figure 6**, both at open circuit (reduced series resistances) and short circuit (higher shunt resistances). During the light soaking, ionic double layers discharge slowly and the ions migrate to the bulk, suppressing interfacial recombination.^[28] As a result and thanks to the sample holder maintained at around 25 °C, the hysteresis was reduced and a PCE as high as 6.6% was achieved after 10 minutes of light soaking. A light soaking longer than 10 minutes did not improve further the performance, as shown by the PV parameters' trend with light soaking time in **Figure S5**. At this point, the module delivered $V_{OC}=19.7$ V (0.895 V per cell) and $I_{SC}=194$ mA (21.6 mA/cm²) with 34.2% FF, suggesting that further improvements will likely originate from improving the latter.

In order to provide a more reliable measurement, the module was held for several seconds at V_{max} until it stabilised at 6.3% PCE, matching the PCE value obtained from the I-V scan. Note that the stabilised value was reached after only a few seconds because it was performed immediately after the I-V scans.

The module also performed well at low light levels under illumination from fluorescent lamps, as reported in Figure 6-c and **Table S2**, yielding around 2 mW at 200 lux (usual indoor illumination level in living rooms), 6 mW at 600 lux (usual indoor illumination level in offices) and 10 mW at 1000 lux (usual indoor illumination level in hypermarkets, for example),^[29] corresponding to 11%, 17% and 18% efficiency, respectively. For comparison, a 5.44 cm² inverted PSC device delivered 340 μ W under 1000 lux from fluorescent lamps.^[30] Focussing on a lighting level of 200 lux from fluorescent lamps, the power density for our module is 10 μ W/cm²; under the same conditions and light source, polycrystalline silicon modules have been reported to yield 2.9 μ W/cm²,^[31] amorphous silicon modules between 3.9^[31] to 5.9 μ W/cm²,^[32] flexible dye sensitised solar modules 2.6^[31] to 2.9 μ W/cm²,^[32] an OPV module of 100 cm² active area delivered up to 9.4 μ W/cm² at 300 lux;^[33] PSCs using SnO₂/MgO electron transport layers generated 20.2 μ W/cm² at 200 lux from LEDs.^[34]

3. Conclusion

A triple mesoporous C-PSC stack fabricated at large scale A4 size modules is demonstrated, using commercially available screen printable pastes and using only 1.6 ml of perovskite solution per module. As expected, patterning the BL improved both V_{OC} and FF thanks to the reduced contact resistance of the Carbon/FTO connection compared to Carbon/BL/FTO. A further improvement came simply by storage in the dark at ambient conditions while no degradation was observed even after hundreds of hours at 70% RH. After 2 months since fabrication, the best module with patterned BL still delivered PCE as high as 6.6% (6.3% stabilised). We believe this to be an important breakthrough on the road to mass production and commercialisation. Work is ongoing to confirm these results on larger batches, assessing process quality and reproducibility, and to increase the still poor geometrical fill factor (45.5%) and the understanding of the physics behind these devices' performance and stability.

4. Experimental Section

A Nd:YVO₄ laser (diode end-pumped, 532 nm wavelength, at 50 kHz average output power 30 W at 200 mm/s, pulse width 10.0 μ s) was used to etch the FTO glass substrates (XOP, TEC 7, 300 mm x 250 mm). The laser patterned substrates were cleaned using Hellmanex detergent (5% in deionised water, rinsed with deionised water, acetone and isopropanol and dried with nitrogen, then plasma cleaned for 10 minutes using a Nano plasma system (Diener Electronics) at 50% of its maximum power. Prior to the cleaning, half of the substrates were completely covered with high temperature Kapton masking tape (RS Pro, 65 μ m) which was then laser cut to mask the areas destined to the series interconnections only and to obtain a patterned compact TiO₂ blocking layer (BL).

The compact TiO₂ BL was deposited in air at ambient conditions by spraying a 0.2 M titanium di-isopropoxide bis(acetylacetonate) solution in isopropanol onto the FTO substrates kept at 180 °C on a hot plate; 25 passes were performed, waiting 40 seconds between sprays

to allow solvent evaporation. The masks made of Kapton tape were removed from the substrates with patterned BL without leaving any residues. All substrates were heated at 300 °C for 15 min and then left to cool down. A commercial TiO₂ paste (Dyesol 30-NRD diluted 1:1 in terpineol) was screen printed and then sintered at 550 °C for 30 min, to obtain an 800 nm-thick mesoporous TiO₂ layer. A 1.2 µm-thick zirconia layer was deposited afterwards by screen printing (Solaronix ZT/SP) and heated at 400 °C for 30 min, followed by the screen printing of the carbon paste (GEM D3) to get a 10 µm-thick top electrode, which was then also annealed at 400 °C for 30 min. The substrates were cooled down and kept at 150 °C until ready for the infiltration of the perovskite solution. All layers were printed in air at ambient conditions.

An equimolar solution of PbI₂ (TCI Chemicals) and MAI (Dyesol) in γ -butyrolactone (Sigma-Aldrich) was prepared adding 5-AVAI (Dyesol) to obtain a 3% molar ratio between 5-AVAI and MAI and drop casted on the modules through the carbon layer, using 8 µl/cm². The infiltration was performed in a low humidity (30% RH) cleanroom to ensure the same ambient conditions for all the modules. After 30 minutes to allow the solution to percolate throughout the triple stack, the modules were annealed in a fan oven for 1 hour and 45 minutes at 50 °C.

The excess of substrate needed for the registration marks was cut, resulting in a final substrate size of 275 mm x 210 mm. Silver paint was applied to obtain busbars and wires soldered to ensure robust contacts on each module.

IV measurements were carried out using in-house developed software and a Keithley 2400 source meter under AM1.5 illumination from a sulphur plasma lamp (Plasma International GmbH) calibrated at 1 sun against a KG5 filtered silicon reference cell (Newport Oriel 91150-KG5). The modules were scanned from V_{OC} to I_{SC} and vice versa at a scan rate of 330 mV/s, after 3 minutes of light soaking. For stabilized measurements, a bias, equal to the voltage at

maximum power determined by the IV sweep, was applied to the device and the current monitored under illumination. The modules were stored in the dark at different values of relative humidity, achieved as follows: for 55% RH, just a closed box stored in a cupboard in the laboratory; for 70% RH, a sealed box with a beaker containing an oversaturated solution of NaCl in water; for 30% RH, a sealed box with silica desiccant on the bottom. Each box had a humidity sensor to monitor the humidity level. While testing the shelf life of C-PSC modules, a more sophisticated system became available: a class AAA solar simulator (Solaronix, Solixon A-20), equipped with thermostatically controlled holder set at 25 °C, was used for all IV measurements from 550 hours after fabrication.

The same software and source meter were used to measure the modules under illumination from compact fluorescent lamps, CFL (Osram L18W/827). The lux levels were measured by a luxmeter (LX-1330B) and the intensity calibrated as in previous work;^[35] the CFL spectrum is reported in Figure S6.

The morphology of films was studied using a JEOL-JSM-7800F field emission scanning electron microscope (5 kV acceleration voltage, a working distance of 10 mm and a magnification of x25,000). Energy dispersive X-ray spectroscopy (EDX) mapping was used to determine the element distribution using 20 kV acceleration voltage.

X-ray diffraction data on the TiO₂ blocking layers sprayed at different temperatures were collected on a D8 Discover (Bruker) X-ray diffractometer with a Cu K α source ($\lambda = 1.5418$ Å) operating at 40 kV and 40 mA. Scans were collected between 10 and 60 degree with a 0.02 degree step. Raman spectroscopy on the same samples was performed with a Renishaw inVia Raman system with a 532 nm laser and 50x objective lens. Spectra were collected with 100% power and 10 accumulations for each sample with 2 seconds/accumulation.

FTO glass substrates (XOP, TEC 7, 57 mm × 57 mm) were used to measure the contact resistance between different layers, namely Carbon/BL/FTO and Carbon/FTO, using the transfer length method (TLM) and the layout reported by Matteocci et al.^[25] A carbon layer was screen printed on both FTO and FTO with sprayed and sintered BL. After annealing at 400 °C for 30 min, resistance (R_{TLM}) between successive printed carbon contacts was measured using a Keithley and the data plotted against the distance between contacts and linearly fitted to extract TLM parameters.

TiO₂ and ZrO₂ were profiled using a Dektak profilometer, with a 12 μg stylus force and 0.333 μm measurement resolution. Layer thickness, average roughness (R_a) and maximum peak height from average thickness (R_p) were calculated over 3 mm for the ZrO₂ and 1 mm for the TiO₂. For the TiO₂ an additional feature (A_p) was measured (as indicated in Fig. S-2) to quantify fully the profile of the layer.

White light interferometry measurements were conducted on the carbon layers using a WYKO NT9300 optical profiling system. A 5x magnification lens was used to measure a 1.22 mm² section incorporating substrate and printed ink edge, a 2-D analysis tool in Vision 32 software was then used to measure ink film thickness as the height difference between cursors placed on the substrate and the ink (avoiding any edge effects and averaged over the 0.94 mm measurement width). Roughness data (R_a and R_p) were recorded using the 2-D analysis after isolating the ink film surface in the measurement.

Supporting Information

Supporting Information is available from the Wiley Online Library or from the author.

Acknowledgements

The authors would like to acknowledge the support provided from the Engineering and Physical Sciences Research Council (EPSRC) through the Self-assembling Perovskite Absorbers - Cells Engineered into Modules project (EP/M015254/1), the PhotoVoltaic

Technology based on Earth-Abundant Materials project (EP/L017792/1) and the SPECIFIC Innovation and Knowledge Centre (EP/N020863/1). The authors would also like to express their gratitude to the Welsh Government for their support of the Sêr Solar programme. DW would like to thank the Sêr Cymru National Research Network for funding of his PhD studies. F.D.R. would like to thank Dr Fabio Matteocci of CHOSE – University of Rome “Tor Vergata” (Italy) for valuable advice on TLM layout and measurements and Dr Adam Pockett from Swansea University for fruitful discussion about hysteresis and ionic movement in perovskite materials.

Received: ((will be filled in by the editorial staff))

Revised: ((will be filled in by the editorial staff))

Published online: ((will be filled in by the editorial staff))

References

- [1] H. Zhang, H. Wang S. T. Williams, D. Xiong, W. Zhang, C.-C. Chueh, W. Chen, A. K.-Y. Jen, *Adv. Mater.*, **2017**, 1606608.
- [2] M. Hu, L. Liu, A. Mei, Y. Yang, T. Liu, H. Han, *J. Mater. Chem. A*, **2014**, 2, (40), 17115–17121.
- [3] Z. Ku, Y. Rong, M. Xu, T. Liu, H. Han, *Sci. Rep.*, **2013**, 3, 3132.
- [4] S. Liu, W. Huang, P. Liao, N. Pootrakulchote, H. Li, J. Lu, J. Li, F. Huang, X. Shai, X. Zhao, Y. Shen, Y.-B. Cheng, M. Wang, *J. Mater. Chem. A*, **2017**, 5(44), 22952-22958.
- [5] W. S. Yang, B.-W. Park, E. H. Jung, N. J. Jeon, Y. C. Kim, D. U. Lee, S. S. Shin, J. Seo, E. K. Kim, J. H. Noh, S. Il Seok, *Science*, **2017**, 356 (6345), 1376–1379.
- [6] A. Mei, X. Li, L. Liu, Z. Ku, T. Liu, Y. Rong, M. Xu, M. Hu, J. Chen, Y. Yang, M. Grätzel, H. Han, *Science*, **2014**, 345, (6194), 295–298.
- [7] G. Grancini, C. Roldán-Carmona, I. Zimmermann, E. Mosconi, X. Lee, D. Martineau, S. Narbey, F. Oswald, F. De Angelis, M. Graetzel, M. K. Nazeeruddin, *Nat. Commun.*, **2017**, 8, 15684.
- [8] S. G. Hashmi, D. Martineau, M. I. Dar, T. T. T. Myllymäki, T. Sarikka, V. Ulla, S. M. Zakeeruddin, M. Grätzel, *J. Mater. Chem. A*, **2017**, 5, (24), 12060–12067.
- [9] K. Domanski, J. P. Correa-Baena, N. Mine, M. K. Nazeeruddin, A. Abate, M. Saliba, W. Tress, A. Hagfeldt, M. Grätzel, *ACS Nano*, **2016**, 10, (6), 6306–6314.
- [10] G. Niu, X. Guo, L. Wang, *J. Mater. Chem. A*, **2015**, 3, (17), 8970–8980.
- [11] S. Razza, F. Di Giacomo, F. Matteocci, L. Cinà, A. L. Palma, S. Casaluci, P. Cameron, A. D’Epifanio, S. Licoccia, A. Reale, T. M. Brown, A. Di Carlo, *J. Power Sources*, **2015**, 277, (2015), 286–291.
- [12] G. Cotella, J. Baker, F. De Rossi, C. Pleydell-Pearce, M. Carnie, T. Watson, *Sol. Energy Mater. Sol. Cells*, **2017**, 159, 362–369.
- [13] J. A. Baker, Y. Mouhamad, K. E. A. Hooper, D. Burkitt, M. Geoghegan, T. M. Watson, *IET Renew. Power Gener.*, **2017**, 11, (5), 546 – 549.

- [14] Y. Hu, S. Si, A. Mei, Y. Rong, H. Liu, X. Li, H. Han, *Sol. RRL*, **2017**, 1600019.
- [15] A. Priyadarshi, L. J. Haur, P. Murray, D. Fu, S. Kulkarni, G. Xing, T. C. Sum, N. Mathews, S. G. Mhaisalkar, *Energy Environ. Sci.*, **2016**, *9*, 3687–3692.
- [16] A. Agresti, S. Pescetelli, A. L. Palma, A. E. D. R. Castillo, D. Konios, G. Kakavelakis, S. Razza, L. Cinà, E. Kymakis, F. Bonaccorso, A. Di Carlo, *ACS Energy Lett.*, **2017**, *2*(1), 279–287.
- [17] J.-S. Yeo, R. Kang, S. Lee, Y.-J. Jeon, N. Myoung, C.-L. Lee, D.-Y. Kim, J.-M. Yun, Y.-H. Seo, S.-S. Kim, S.-I. Na, *Nano Energy*, **2015**, *12*, 96–104.
- [18] *China, Microquanta Co. Ltd. Hangzhou*, 2017. [Online]. Available: <http://2107081062.wezhan.us/newsitem/277909853>. [Accessed: 05-Apr-2018].
- [19] M. A. Green, Y. Hishikawa, W. Warta, E. D. Dunlop, D. H. Levi, J. Hohl-Ebinger, A. W. H. Ho-Baillie, *Prog. Photovoltaics Res. Appl.*, **2017**, *25*, (7), 668–676.
- [20] A. L. Palma, F. Matteocci, A. Agresti, S. Pescetelli, E. Calabro, L. Vesce, S. Christiansen, M. Schmidt, A. Di Carlo, *IEEE J. Photovoltaics*, **2017**, *7*, (6), 1674–1680.
- [21] J. Troughton, K. Hooper, T. M. Watson, *Nano Energy*, **2017**, *39*, 60–68.
- [22] Y. Galagan, E.W.C. Coenen, W.J.H. Verhees, R. Andriessen, *J. Mater. Chem. A*, **2016**, *4*, 5700-5705
- [23] J. Baker, K. Hooper, S. Meroni, A. Pockett, J. McGettrick, Z. Wei, R. Escalante, G. Oskam, M. Carnie, T. Watson, *J. Mater. Chem. A*, **2017**, 18643–18650.
- [24] S. M. P. Meroni, Y. Mouhamad, F. De Rossi, A. Pockett, J. Baker, R. Escalante, J. Searle, M. J. Carnie, E. Jewell, G. Oskam, T. M. Watson, *Sci. Technol. Adv. Mater.*, **2018**, *19*, (1), 1–9.
- [25] F. Matteocci, L. Cina, F. Di Giacomo, S. Razza, A.L. Palma, A. Guidobaldi, A. D’Epifanio, S. Licoccia, T.M. Brown, *Prog. Photovoltaics Res. Appl.*, **2014**, *24* (4), 436–445.
- [26] P. Calado, A. M. Telford, D. Bryant, X. Li, J. Nelson, B. C. O’Regan, P. R. F. Barnes, *Nat. Commun.*, **2016**, *7*, 13831.
- [27] D. Bryant, S. Wheeler, B. C. O’Regan, T. Watson, P. R. F. Barnes, D. Worsley, J. Durrant, *J. Phys. Chem. Lett.*, **2015**, *6*, (16), 3190–3194.
- [28] A. Pockett, M. Carnie, *ACS Energy Lett.*, **2017**, *2*, 1683-1689
- [29] *UK Society of Light and Lighting, Code for Lighting*, **2012**, <https://www.cibse.org/knowledge/knowledge-items/detail?id=a0q20000008I6xiAAC>. [Accessed: 14-Jun-2018].
- [30] C.-Y. Chen, J.-H. Chang, K.-M. Chiang, H.-L. Lin, S.-Y. Hsiao, H.-W. Lin, *Adv. Funct. Mater.*, **2015**, *25* (45), 7064-7070.
- [31] Y. Li, N. J. Grabham, S. P. Beeby, M. J. Tudor, *Sol. Energy*, **2015**, *111*, 21–29.
- [32] F. De Rossi, T. Pontecorvo, T. M. Brown, *Applied Energy*, **2015**, *156*, 413-422.
- [33] H. K. H. Lee, Z. Li, J. R. Durrant, W. C. Tsoi, *Applied Physics Letters*, **2016**, *108*, 253301.
- [34] J. Dagar, S. Castro-Hermosa, G. Lucarelli, F. Cacialli, T. M. Brown, *Nano En.*, **2018**, *49*, 290-

299.

- [35] J. A. Baker, C. Worsley, H. K. H. Lee, R. N. Clark, W. C. Tsoi, G. Williams, D. A. Worsley, D. T. Gethin, T. M. Watson, *Adv. Eng. Mater.*, **2017**, 1600652.

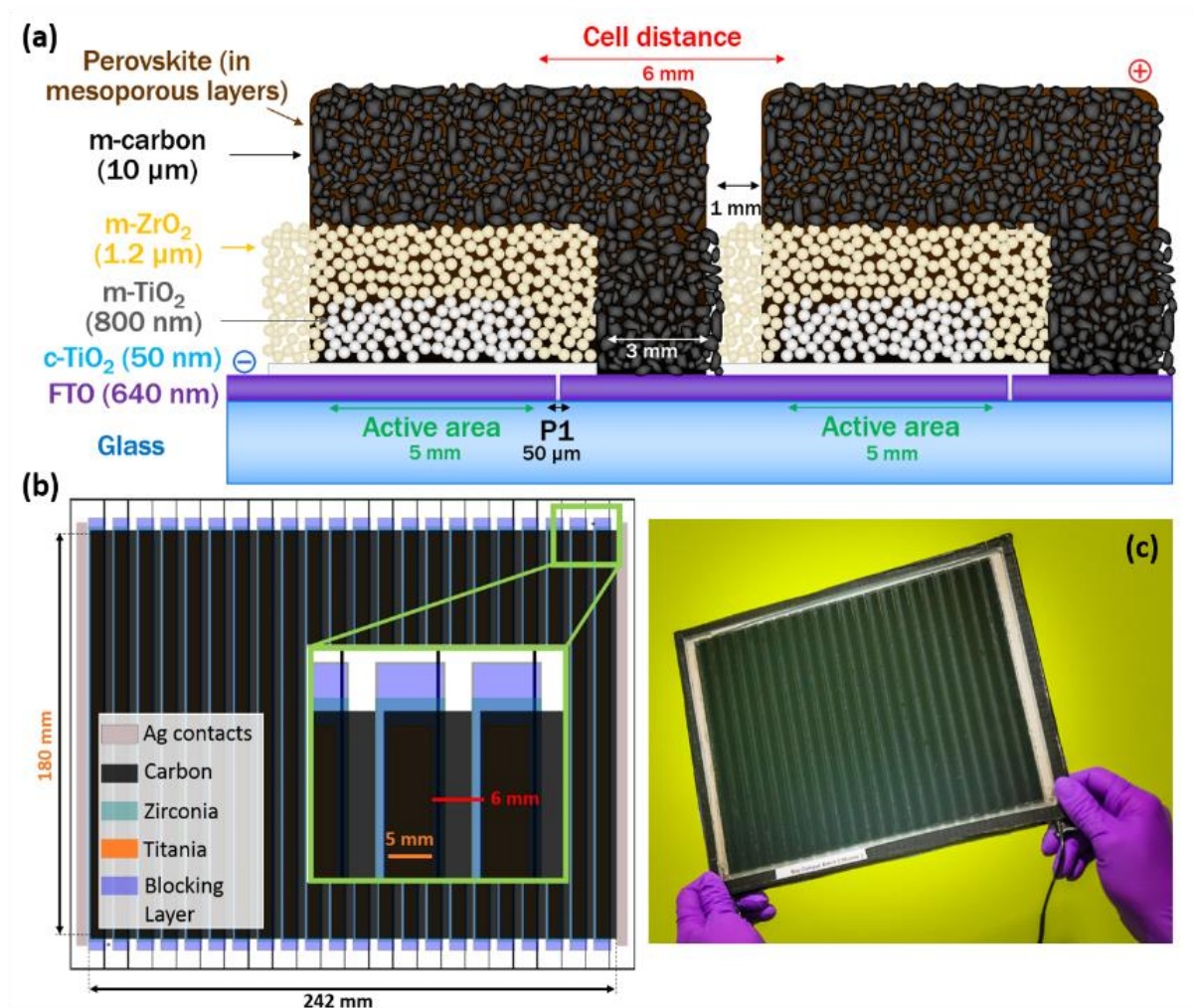


Figure 1. (a) Cross-section schematics of adjacent cells in the module with nominal thickness of each layer, highlighting the laser-etched FTO, patterning of TiO₂ blocking layer and the electrical vertical connection, ensured by the carbon back contact. (b) Module schematics, showing the different overlapping layers, the dimensions of the active area for both the individual single cell and the whole module as well as the distance between adjacent cells (inset). (c) Photo of a module; wires have been soldered to the silver painted busbars to provide more robust electrical contacts.

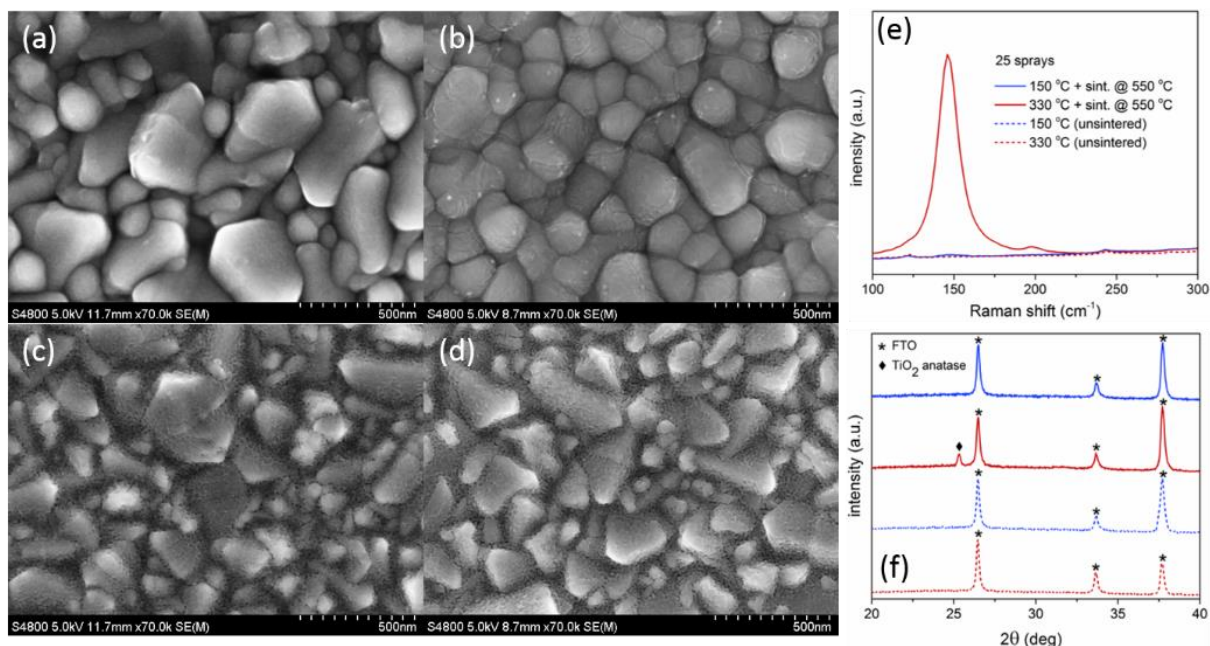


Figure 2. SEM images of TiO₂ compact layers, sprayed at 300 °C, (a) before and (b) after sintering at 550 °C for 30 min and sprayed at 150 °C, (c) before and (d) after sintering at 550 °C for 30 min. (e) Raman and (f) XRD spectra, showing the characteristic anatase peak respectively at 145 cm⁻¹ and 25.3 degrees.

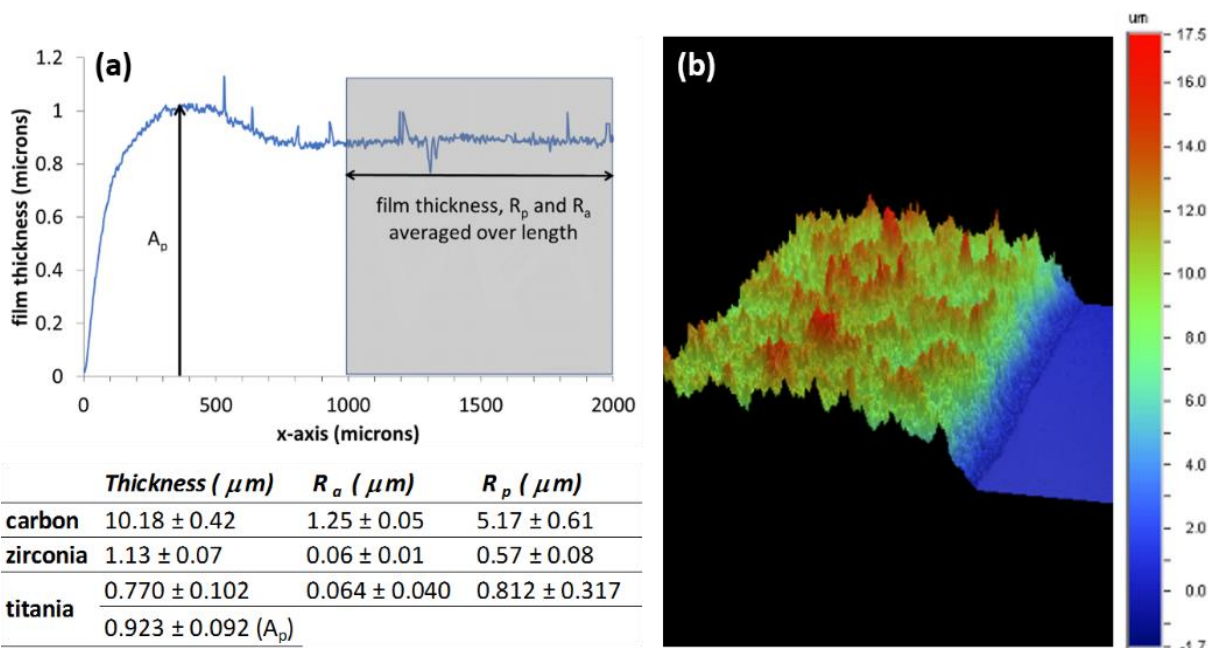


Figure 3. Profile of TiO₂ layer, showing how A_p was measured to consider the different heights recorded at the edges and in the central part of the film; (b) white light interferometry of the carbon layer, revealing its significant roughness. Average values for thickness, average roughness R_a and peak roughness R_p are reported in the table.

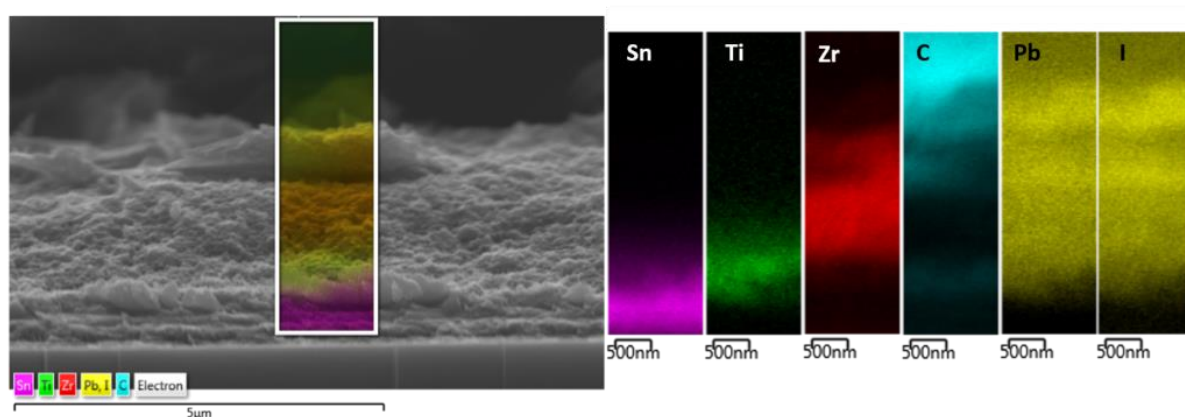


Figure 4. Cross-section SEM image of one individual cell out the module and EDX maps for the elements, Sn (indicating the FTO conductive layer), Ti (indicating the porous TiO₂ electron transport layer), Zr (indicating the porous insulating ZrO₂ layer), C (indicating the porous graphite/carbon black top electrode), Pb and I (indicating the infiltrated perovskite throughout the stack).

Table 1. Average PV parameters for modules with un-patterned and patterned BL (2 modules per type) after the infiltration and annealing of the perovskite (0 h), after 144 hours of storage in the dark at ambient conditions, i.e. room temperature and 55% RH, and after further 48 hours at 70% RH.

Un-patterned BL		V _{oc} [V]	st.dev.	I _{sc} [mA]	st.dev.	FF [%]	st.dev.	PCE [%]	st.dev.
0 h	rev	16.3	0.9	78.1	9.3	29.2	6.2	1.9	0.7
	fwd	15.0	0.8	75.7	10.0	27.9	7.0	1.7	0.6
144 h at 55% RH	rev	16.1	1.4	98.6	2.9	26.7	7.2	2.2	1.6
	fwd	15.9	2.0	97.1	0.8	20.4	0.8	1.6	0.3
144 h at 55% RH + 48 h at 70% RH	rev	16.2	1.4	98.2	11.0	27.3	8.8	2.3	1.1
	fwd	15.6	2.2	97.0	8.9	21.6	1.4	1.7	0.5
Patterned BL		V _{oc} [V]	st.dev.	I _{sc} [mA]	st.dev.	FF [%]	st.dev.	PCE [%]	st.dev.
0 h	rev	18.2	0.1	91.0	19.3	38.9	4.2	3.2	0.3
	fwd	17.6	0.4	91.2	19.7	28.6	9.5	2.2	0.3
144 h at 55% RH	rev	18.0	0.2	107.4	3.9	37.2	1.7	3.6	0.3
	fwd	17.2	0.1	107.1	2.8	25.4	5.0	2.4	0.5
144 h at 55% RH + 48 h at 70% RH	rev	19.2	0.1	110.0	8.9	39.6	1.3	4.2	0.5
	fwd	18.2	0.5	109.8	9.2	25.8	1.4	2.6	0.1

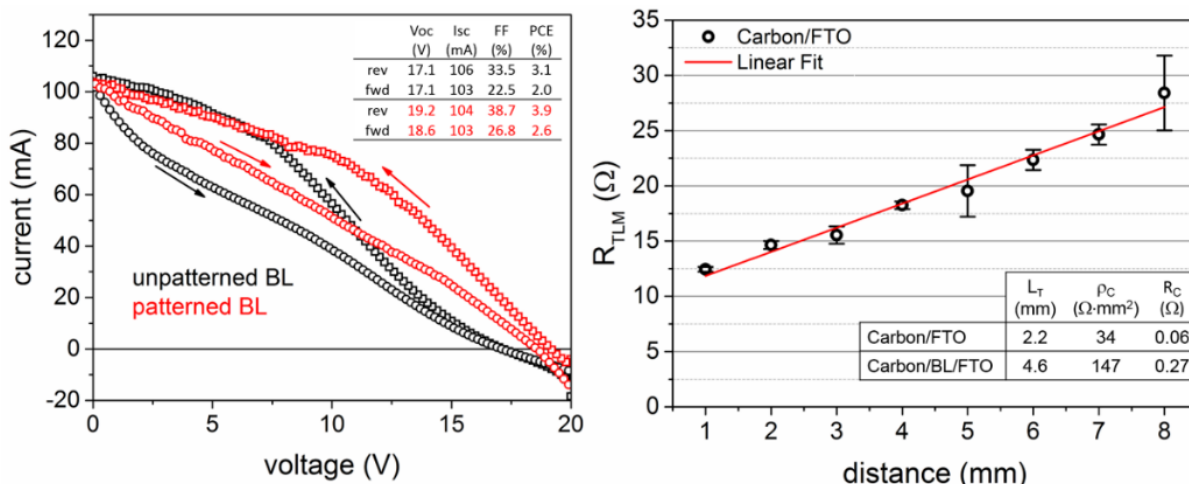


Figure 5. IV curves for the best modules with un-patterned and patterned BL (after 144 hours at ambient conditions and 48 hours of 70% RH treatment, left), showing the improvement in the curve shape, mainly due to lower series resistances and higher FF; measured TLM resistance values varying the contact distance (right) when the carbon is directly contacting the FTO, i.e. when the BL is patterned, and TLM parameters (inset table), namely transfer length (L_T), contact resistivity (ρ_C) and contact resistance (R_C , using 540 mm^2 contact area) for patterned BL (Carbon/FTO) and un-patterned BL (Carbon/BL/FTO, measured values and linear fit not shown here because out of scale – see **Figure S3**).

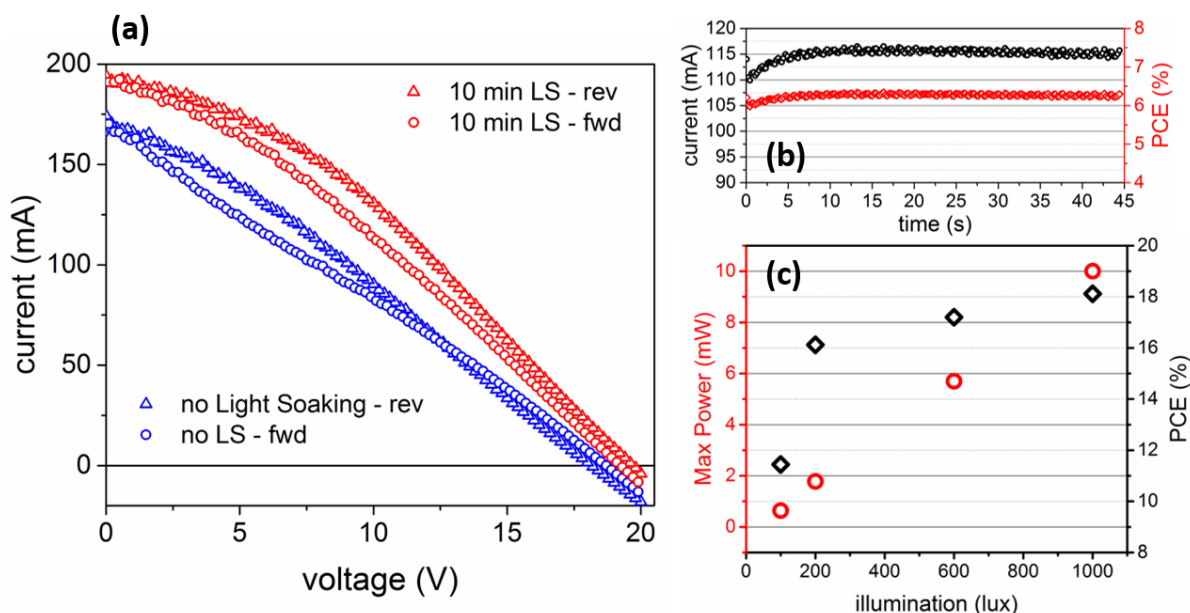


Figure 6. (a), (b) Effect of light soaking at open circuit prior to the I-V scans for the best module with patterned BL, after over 2 months since its fabrication and using a thermostatically controlled holder set at $25 \text{ }^\circ\text{C}$: (a) I-V curves in both scan directions without any light soaking and after 10 minutes of light soaking and (b) output current stabilised over time at $V_{\text{max}}=10.8 \text{ V}$. (c) Maximum output power and PCE (reverse scan only) of best module

with patterned BL at different illumination levels under fluorescent lamps. I-V curves are shown in **Error! Reference source not found.**

Table 2. PV parameters of the best modules with patterned BL, after over 2 months since its fabrication and using a thermostatically controlled holder set at 25 °C, showing the effect of light soaking at open circuit prior to I-V scans.

	V_{oc} [V]		I_{sc} [mA]		FF [%]		PCE [%]	
	No LS	10 min LS	No LS	10 min LS	No LS	10 min LS	No LS	10 min LS
rev	18.2	19.7	173	192	28.9	34.2	4.6	6.6
fwd	18.7	19.2	168	194	26.5	30.8	4.2	5.7

Low cost materials and equipment are used to demonstrate large area screen printed perovskite solar modules, advancing the route to commercialization of these solution processed devices. The screen printing process is optimized to avoid defects caused by printing such large areas. The resulting module with an efficiency of 6.3% is world leading for a device of this size.

Keyword perovskite solar cells, modules, carbon, mesoporous, printed

F. De Rossi, J. Baker, D. Beynon, K. Hooper, S. Meroni, D. Williams, Z. Wei, A. Yasin, C. Charbonneau, E. Jewell, and T. M. Watson

All printable perovskite solar modules with 198 cm² active area and over 6% efficiency

ToC figure

